Frequency driven inversion of tunnel magnetoimpedance and observation of positive tunnel magnetocapacitance in magnetic tunnel junctions

Subir Parui, Mário Ribeiro, Ainhoa Atxabal, Amilcar Bedoya-Pinto, Xiangnan Sun, Roger Llopis, Fèlix Casanova, and Luis E. Hueso

Citation: Applied Physics Letters **109**, 052401 (2016); doi: 10.1063/1.4960202
View online: http://dx.doi.org/10.1063/1.4960202
View Table of Contents: http://scitation.aip.org/content/aip/journal/apl/109/5?ver=pdfcov
Published by the AIP Publishing

Frequency driven inversion of tunnel magnetoimpedance and observation of positive tunnel magnetocapacitance in magnetic tunnel junctions

Subir Parui,[1,a)] Mário Ribeiro,[1] Ainhoa Atxabal,[1] Amilcar Bedoya-Pinto,[1,2] Xiangnan Sun,[1,3] Roger Llopis,[1] Fèlix Casanova,[1,4] and Luis E. Hueso[1,4,a)]
[1]*CIC nanoGUNE, 20018 Donostia-San Sebastian, Spain*
[2]*Max Planck Institute of Microstructure Physics, D-06120 Halle, Germany*
[3]*National Center for Nanoscience and Technology, 100190 Beijing, People's Republic of China*
[4]*IKERBASQUE, Basque Foundation for Science, 48011 Bilbao, Spain*

(Received 26 May 2016; accepted 21 July 2016; published online 1 August 2016)

The relevance for modern computation of non-volatile high-frequency memories makes ac-transport measurements of magnetic tunnel junctions (MTJs) crucial for exploring this regime. Here, we demonstrate a frequency-mediated effect in which the tunnel magnetoimpedance reverses its sign in a classical $Co/Al_2O_3/NiFe$ MTJ, whereas we only observe a gradual decrease in the tunnel magnetophase. Such effects are explained by the capacitive coupling of a parallel resistor and capacitor in the equivalent circuit model of the MTJ. Furthermore, we report a positive tunnel magnetocapacitance effect, suggesting the presence of a spin-capacitance at the two ferromagnet/tunnel-barrier interfaces. Our results are important for understanding spin transport phenomena at the high frequency regime in which the spin-polarized charge accumulation due to spin-dependent penetration depth at the two interfaces plays a crucial role. *Published by AIP Publishing.*
[http://dx.doi.org/10.1063/1.4960202]

Magnetic random access memory (MRAM) devices based on magnetic tunnel junctions (MTJ) are very attractive technologically, mostly due to their low energy consumption and fast data processing.[1–5] The two-terminal geometry of the MTJs is based on a thin dielectric layer (I) acting as the tunnel barrier, sandwiched between two ferromagnetic electrodes (FM), in a FM/I/FM structure.[1–5] MTJs typically show low (/high) resistance states when the magnetic orientation of the two ferromagnetic electrodes is parallel (/antiparallel), providing a positive tunnel magnetoresistance (TMR).[1–7] Beyond this conventional positive TMR effect, there are several non-trivial effects that give rise to negative TMR, where the low (/high) resistance states now correspond to the antiparallel (/parallel) orientation of the electrodes' magnetization, namely, spin-polarized resonance,[8] quantum size effects,[9] modulation of the density-of-states (DOS) of the ferromagnetic electrodes,[10] inversion of tunneling spin polarization at the FM/I interface,[11] and the formation of a tunneling standing wave.[12] These mechanisms are usually addressed by either dc (direct current) or ac (alternating current)-transport measurements at low frequencies.[12,13] For ac measurements, the impedance (Z), i.e., the total dynamic resistance of the circuit converges to the resistance measured only with dc-voltages when the phase shift (θ) is negligible. Phenomena such as spin polarized resonant tunneling, in which the TMR changes from positive to negative, is crucial for the development of resonant-tunneling spin transistors and quantum information devices.[8] However, so far, this effect has been shown to occur when the thickness of a metallic insertion layer (Cu) between the FM and I layers is varied within a certain range.[8] Accordingly, it would be important to have alternative ways for controlling the magnetoimpedance (or magnetoresistance) externally that does not depend on the structural characteristics of the device. At the same time, it will be interesting to explore new phenomenon related to spin-capacitance based on the analysis of impedance spectroscopy measurements.

Here, we demonstrate a controlled positive-to-negative inversion of the tunnel magnetoimpedance with increasing frequencies in a classical $Co/Al_2O_3/NiFe$ MTJ by using impedance-spectroscopy measurements. The magnitude of the inversion depends on the individual resistance change between parallel and antiparallel magnetic states and the change in the spin-capacitance[14] of the FM/I interfacial layer. Simultaneously, the impedance-spectroscopy measurements not only help us to determine the presence of spin-capacitance but also to characterize the speed of the device operation, and to estimate the tunnel magnetocapacitance effect.[15–19] We report a positive tunnel magnetocapacitance using a simple parallel equivalent circuit of a resistor and a capacitor of the MTJ, and by measuring the impedance and phase at set frequencies. In the regime of frequencies where the equivalent parallel circuit model is reliable, the tunnel magnetoresistance measured by ac-method comes in agreement with the dc-measurements. Our results open the possibility to exploit the impedance-spectroscopy measurements for the optimization of functional spintronic devices.

A vertical cross-bar geometry of Co (16 nm)/Al_2O_3 (x nm)/$Ni_{80}Fe_{20}$ (16 nm) (from bottom to top, see Figure 1) was deposited *in situ* through different shadow masks. The junction stack is fabricated on a Si/SiO_2 (150 nm) substrate. Initially, several 16-nm-thick Co bars are deposited by e-beam evaporation in an ultrahigh vacuum (UHV) chamber at the rate of 1 Å/s. Afterwards, the Al_2O_3 tunnel barrier is obtained evaporating Al (2.5 or 3 nm) all over the device, followed by plasma oxidation. Two steps of plasma oxidation at the oxygen pressure of 10^{-1} mbar are employed in order to obtain a

a)Electronic addresses: s.parui@nanogune.eu and l.hueso@nanogune.eu

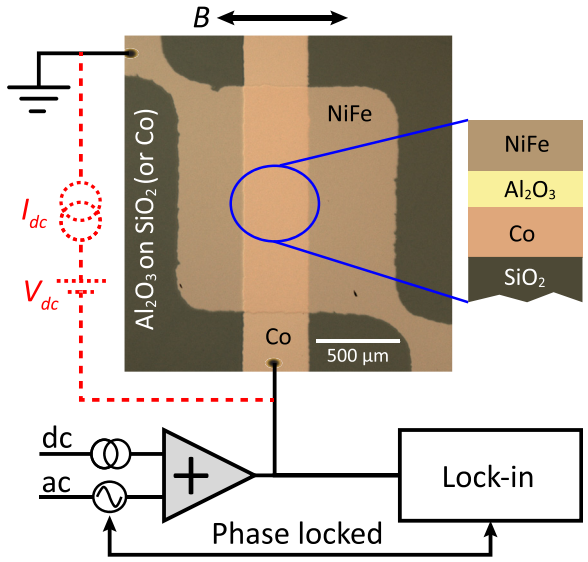

FIG. 1. Optical microscopy image of the device and the schematic diagram of the MTJ of $Co/Al_2O_3/NiFe$ stacked on a Si/SiO_2 substrate. The dotted red-line represents the standard two-probe dc measurement schematics, and the solid black-line represents the schematics of the impedance-spectroscopy measurement. Sweeping direction of the applied magnetic field B is also shown.

robust Al_2O_3 tunnel barrier.[20] Finally, a 16-nm-thick NiFe top electrode was deposited at the rate of 1 Å/s through a different shadow mask. The active area for tunneling is considered to be confined to the overlapping area between the Co bar and the NiFe bar (here, we report results from two different device areas of 0.5 and 0.2 mm^2). The Al_2O_3 dielectric sandwiched between the two ferromagnetic electrodes also provides a two terminal capacitor. Once fabricated, the device is transferred into a variable-temperature probe station (Lakeshore) for electrical measurements with a Keithley-4200 CVU semiconductor analyzer, which is capable to carry out both the impedance-spectroscopy measurement in the frequency range of 10^3–10^7 Hz and the standard dc measurements. Using a two-probe configuration, we measure both types of transport characteristics using the same two probes to avoid any circuit complication in the high frequency operation.[19] In Figure 1, the dotted line (red) shows the standard dc measurement schematics, and the solid line (black) represents the schematics of the impedance-spectroscopy (ac + dc) measurement.

We first focus on the standard dc-transport measurements of the MTJs (see supplementary material, Figure S1[21]). In the case of a thin tunnel barrier, the s- and d-orbital electrons that tunnel from one ferromagnet to the other conserve the spin information via the single-step tunnel process.[22] The transport can be described as having two independent spin channels of two different resistances. In general, a low resistance state is observed for parallel alignment (R_P) of the two ferromagnets, and a high resistance state (R_{AP}) is observed when they are anti-parallel. The associated tunneling magnetoresistance (TMR_{DC}) ratio is defined as

$$TMR_{DC} = \frac{(R_{AP} - R_P)}{R_P} \times 100. \quad (1)$$

The electric resistance of the parallel and anti-parallel magnetic states of the device is measured by two-probe method with the applied dc voltage up to ±600 mV. The TMR_{DC} in the MTJ reaches 20% at the lowest temperatures, at +10 mV of dc bias. Increasing the bias voltage increases the spin relaxation rate, which decreases the TMR_{DC} as the electrons tunnel into empty states of the receiving electrode with an excess energy, generating phonons and magnons.[23,24] Nevertheless, these values of TMR_{DC} is comparable to previous literature,[1,7,23] confirming the good quality of our MTJs with the characteristics of the direct tunneling process between the two ferromagnetic materials.

In order to investigate the tunnel magnetoimpedance effect, we focus on the impedance-spectroscopy measurement combining an ac bias with an applied dc bias. From the ac-transport measurement, we obtain the impedance and the phase (Z, θ) as the fundamental parameters. From Z and θ, we can obtain $Re(Z) = |Z| \cos\theta$ and $Im(Z) = |Z| \sin\theta$, where $Z = Re(Z) + iIm(Z)$ and $|Z| = \sqrt{Re(Z)^2 + Im(Z)^2}$. We must note that both Z and Re(Z) converge to the dc value of the resistance in the case of $\theta \to 0°$ at the low frequency regime, so that $|Z| \approx Re(Z) \approx R_{DC}$ and the system is resistive. However, the system follows capacitive behavior at the frequencies where θ approaches to −90°.

Figure 2 represents (Z, θ) and [Re(Z), Im(Z)] as a function of the magnetic field for two different frequencies, 2 kHz and 30 kHz, respectively, for the same MTJ as discussed in the dc-transport measurement. The black (left axis) and the red (right axis) arrows are used to indicate Z, Re(Z) and θ, Im(Z), respectively. Comparing these two frequencies, we see that the switching of both Z and Re(Z) (black curves) becomes inverted, whereas θ and X (red curves) remain consistent with their usual switching behavior. It is worth noting that the overall Z and Re(Z) value decreases at 30 kHz compared to the frequency at 2 kHz. However, an increase of θ and Im(Z) suggests the presence of the capacitive coupling in the device. Nevertheless, the switching behaviors of Z and Re(Z) with respect to the magnetic field clearly confirm the frequency-driven inversion of tunnel magnetoimpedance in the MTJ.

In order to identify the different frequency regimes for positive and negative tunnel magnetoimpedance, we performed frequency scans of Z and θ for parallel and antiparallel magnetic orientations, respectively. Figure 3 shows the frequency-dependence of Z, θ, TMZ, and TMθ, respectively. We calculate TMZ and TMθ by using the same formula as in Equation (1) but by changing the respective parameters (Z and θ). Figure 3(c) shows that the TMZ converges to the TMR_{DC} values in the low frequency regime of ∼1 kHz. Due to the capacitive coupling that originates from the charge accumulation at the two interfaces between the ferromagnets and the Al_2O_3 dielectric, both the TMZ and TMθ values decrease with increasing frequency. The damping of the frequency response depends on the frequency independent resistance and the capacitance of the MTJ, which can also be further controlled by engineering the MTJs, as will be discussed below. Nevertheless, the TMZ values [see Figure 3(c)] flip their sign in the frequency range of $\sim 2 \times 10^4$ to $\sim 2 \times 10^5$ Hz before reaching zero, and such inversion phenomena is in agreement with the earlier study.[25] Here, we propose that the inversion of TMZ is related to the quicker

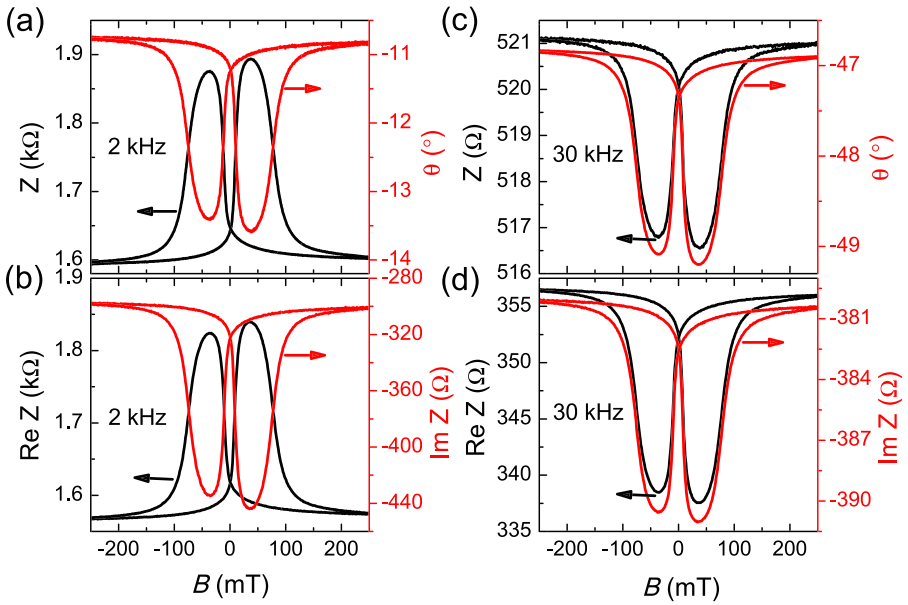

FIG. 2. (a) and (b) Magnetic field dependent (Z, θ), and [Re(Z), Im(Z)], respectively, at 2 kHz. Measurements are performed individually at +10 mV of dc bias, 30 mV of RMS ac bias, and at 10 K. (c) and (d) Similar measurements as in (a) and (b) are now performed at 30 kHz. At this frequency, the switching of Z and Re(Z) is inverted.

damping of Z in the AP state relative to the P state as a function of the frequency. This can be understood on the basis of different resistances and capacitances in the AP and P states resulting in different time constants, which eventually control the damping of Z and of its inversion.

It is possible to interpret the impedance-spectroscopy measurements via an equivalent circuit model (see supplementary material, Figure S2[21]). In MTJs, the resistance and capacitance are coupled in a parallel equivalent circuit.[15–19] The Cole-Cole plots between Re(Z) and Im(Z) show semicircular dependences, which validate the parallel circuit model.[18,19] In order to simplify the circuit analysis and to determine the respective frequency (f) independent static resistance (R_f) and static capacitance (C_f), the magnetic field independent part during ac-measurement can be eliminated by taking the difference of the impedances in the P and AP states.[18] This difference can be written as $\Delta Z = \Delta \mathrm{Re}(Z) + i\Delta \mathrm{Im}(Z)$, where

$$\Delta Re(Z) = \left(\frac{R_f(AP)}{1 + 4\pi^2 f^2 R_f^2(AP) C_f^2(AP)} - \frac{R_f(P)}{1 + 4\pi^2 f^2 R_f^2(P) C_f^2(P)} \right), \tag{2}$$

$$\Delta Im(Z) = -2\pi f \left(\frac{C_f(AP) R_f^2(AP)}{1 + 4\pi^2 f^2 R_f^2(AP) C_f^2(AP)} - \frac{C_f(P) R_f^2(P)}{1 + 4\pi^2 f^2 R_f^2(P) C_f^2(P)} \right). \tag{3}$$

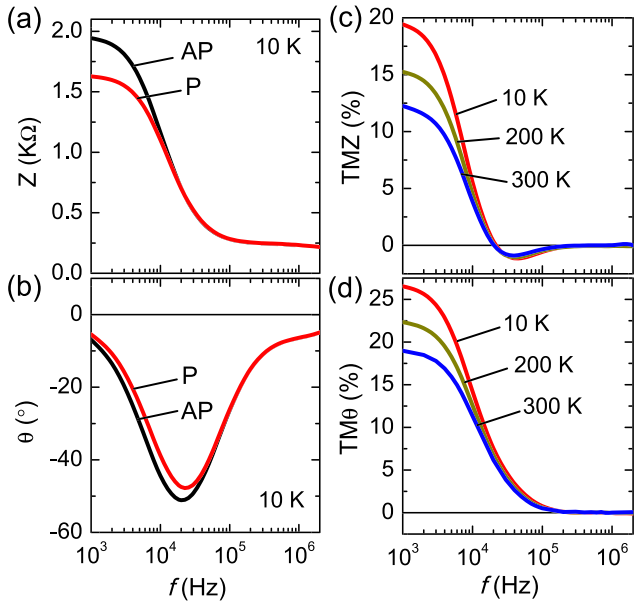

FIG. 3. (a) Impedance and (b) phase as a function of frequency at 10 K for the P and AP orientations of the magnetization of the two FM electrodes. All the two-probe impedance-spectroscopy measurements are carried out at dc bias of +10 mV and at RMS ac bias of 30 mV. (c) Tunneling magnetoimpedance (TMZ) and (d) tunneling magnetophase (TMθ) as a function of frequency at different temperatures.

From the extracted fitting parameters (see supplementary material, Table SI[21]), we observe that the positive tunnel magnetoresistance (~23% at 10 K) is consistent with the dc measurements, whereas almost no tunnel magnetocapacitance effect is extracted. This result coincides with a previous report,[17] although it is fair to admit the conflicting studies in this regard.[15,16,18,19]

The temperature independent capacitance values extracted from these fittings amount to 12.7 nF. By considering the parallel plate capacitor device structure of our MTJs, we calculate the geometrical-capacitance ($C_g = \varepsilon \frac{A}{d}$) to be 10.2 nF, where A is the area of the junction (0.5 mm^2), d is the thickness (3-nm-thick Al yields an Al_2O_3 tunnel barrier of 3.9 nm as $d_{Al_2O_3} \approx 1.3 d_{Al}$[26]), and ε is the dielectric constant of Al_2O_3 ($9\varepsilon_0$, $\varepsilon_0 = 8.85 \times 10^{-12}$ F/m). The capacitance extracted from the fit is slightly larger than the geometrical capacitance, which suggests the presence of an additional leaky capacitance in parallel to the geometrical capacitance,[18] making the model unreliable for the detection of interface spin capacitance. Below we discuss a straightforward approach to detect the influence of the two interface spin-capacitances which are in principle in series with the geometrical capacitance,[16,18] and give rise to the positive tunnel magnetocapacitance.

In a parallel resistor-capacitor circuit model, the time constant is determined as the product of the corresponding resistance and capacitance. Such time constant of MTJs plays an important role for high-speed applications. From our large area tunnel junction, we determine the time constants to be of the order of μs. However, the time constant of the circuit changes in two different magnetic configurations (P and AP) as well as in different temperatures due to the change in resistance in the circuit. A cutoff frequency $f_c = \frac{1}{2\pi R_f C_f}$ can thus be obtained. For example, the cut-off frequencies at 10 K are 7.3 kHz (AP-state) and 8.9 kHz (P-state), respectively. Interestingly, these cut-off frequencies are quite close to the frequency regime above which we observe the inversion of TMZ as can be seen in Figure 3(c).

Further, we perform a more straightforward analysis to determine the frequency dependent resistance and the capacitance.[15,16] Considering the MTJ as a parallel network of r and c, we calculate their values directly at each set frequency from the (Z, θ) measurements. The direct dependence can be expressed as follows: $r = Z\sqrt{1 + (\tan\theta)^2}$ and $c = (Z\omega)^{-1}[1 + (\tan\theta)^{-2}]^{-1/2}$, where $\omega = 2\pi f$ is the frequency of the ac signal. Figure 4(a) shows the typical c and r dependence with varying magnetic fields. Our measurement shows a positive TMc value, smaller than the positive TMr values. The positive value of TMc indicates that there is higher capacitance in the AP-state than in the P-state. We must note that a positive TMc is observed in an asymmetric MTJ, whereas earlier studies report a negative tunnel magnetocapacitance in symmetric MTJs with identical ferromagnetic electrodes.[15,16,18,19] We suggest that one of the possible mechanisms behind the positive TMc is the different spin-dependent screening length of the spin polarized charge accumulation at the two different FM/I interface (Co/Al_2O_3 and $NiFe/Al_2O_3$). Figure 4(b) reveals the dc-bias dependence of the normalized TMr and TMc during the impedance-spectroscopy measurements. We observe a decrease with increasing bias for both magnitudes, which is consistent with standard dc measurements. We also observe that the TMc is relatively less sensitive to the applied dc-bias than the TMr, indicating a low leakage current in the MTJ.[18] Figures 4(c) and 4(d) show the frequency dependence of the TMr and TMc at different temperatures. In an ideal case, TMr and TMc are expected to be frequency independent. However, TMr and TMc decrease very sharply after a certain frequency, and we also notice a weak inversion in TMr. Nevertheless, in the low frequency regime, we observe an almost temperature independent TMc, whereas the TMr is very consistent with the standard dc-measurements at different temperatures.

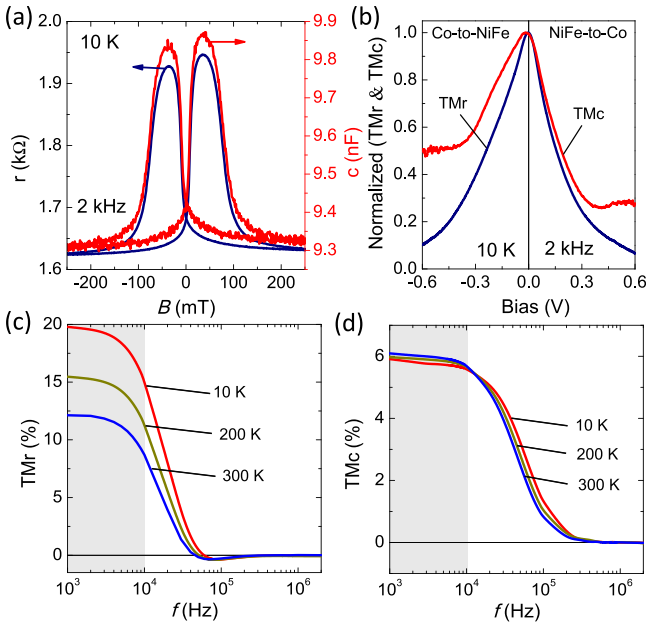

FIG. 4. (a) The magnetic field dependence of resistance (r) and capacitance (c) of the MTJ by considering the parallel equivalent circuit. The measurements are done at dc bias of +10 mV and at RMS ac bias of 30 mV. (b) Normalized bias dependence of both TMr and TMc of the device. Frequency dependence of the TMr (c) and TMc (d) is shown at different temperatures.

An in-plane magnetic field dependence of the capacitance of a parallel plate capacitor can be induced via a combination of the Lorentz force and quantum confinement effects[27,28] or by spin-dependent Zeeman splitting.[29,30] Such phenomena are named as *magnetocapacitance* effect in a system without any ferromagnetic electrode. However, the origin of tunnel magnetocapacitance in MTJs can only be attributed to the presence of spin-capacitance at the two FM/I interface that appears due to the capacitive accumulation of spin-polarized carriers at the interface.[14]

In order to have further control over the inversion phenomena in the tunnel magnetoimpedance, it is thus also important to have a different frequency response of the MTJs (see supplementary material, Figure S3[21]). Since the tunnel resistance is bias dependent, it is expected to have a change in the frequency response and also in the amplitude of inversion of the tunnel magnetoimpedance. The TMZ shows a sharply damped oscillation and an increase in the frequency response of damping with increasing dc-bias. However, none of the TMθ plots show inversion. Furthermore, a modification in the thickness of the tunnel barrier and/or the area of the overlapping electrodes in the MTJ can be used to tune the damping frequency. In the case of the thinner tunnel barrier, the resistance of the junction decreases exponentially with decreasing thickness, whereas the capacitance increases, since it is inversely proportional to the thickness between the two electrodes. Thus, for the tunnel barrier from 2.5-nm-thick Al, we observe the cut off frequency of the inversion increases compared to the junction with the tunnel barrier from 3-nm-thick Al and such observation of frequency shift is in agreement with the previous literature.[16] Furthermore, both the tunnel resistance and the capacitance change with the effective device area, and we observe higher frequency shift of the inversion with decreasing device area. Consequently, we confirm that the inversion in tunnel magnetoimpedance is very robust and easily tunable by applied dc bias and/or by engineering the junction geometrical parameters.

In conclusion, we demonstrate an alternative mechanism to achieve inversion in the tunnel magnetoimpedance of MTJs, based on the frequency of the applied ac-signal. Ac-transport measurements of the impedance and corresponding phase allow the extraction of other fundamental parameters, such as resistance and capacitance. From the straightforward determination of the equivalent resistance and capacitance, we

determine not only a positive tunnel magnetoresistance but also a positive tunnel magnetocapacitance effect. Moreover, in order to establish the robustness of the inversion phenomena, we report the dependence of the frequency response of the magnetoimpedance with the dc bias-voltage, thickness of the tunnel barrier, and area of the two overlapping electrodes of the MTJs. Our results are encouraging to understand the spin-polarized charge accumulation as well as spin transport phenomena in spintronic devices at high frequencies involving any thin dielectric tunnel barrier, including ferromagnetic insulators. In particular, the inversion phenomena in MTJs will help extending the current use of Al_2O_3 tunnel barriers in hot electron transistors[31,32] as well as encourage the development of highly functional spin transport devices.

We are grateful to Professor Hanan Dery for useful discussions. We also acknowledge financial support from the European Union's 7th Framework Programme under the European Research Council (Grant No. 257654-SPINTROS), under People Programme (Marie Curie Actions) REA Grant Agreement No. 607904-13, SPINOGRAPH, the Basque Government for a PhD fellowship (PRE_2015_2_0139), and under the NMP project (NMP3-SL-2011-263104- HINTS) as well as by the Spanish Ministry of Economy under Project No. MAT2015-65159-R.

[1]J. S. Moodera, L. R. Kinder, T. M. Wong, and R. Meservey, Phys. Rev. Lett. **74**, 3273 (1995).
[2]S. Parkin, X. Jiang, C. Kaiser, A. Panchula, K. Roche, and M. Samant, Proc. IEEE **91**, 661 (2003).
[3]S. S. P. Parkin, C. Kaiser, A. Panchula, P. M. Rice, B. Hughes, M. Samant, and S.-H. Yang, Nat. Mater. **3**, 862 (2004).
[4]S. Yuasa, T. Nagahama, A. Fukushima, Y. Suzuki, and K. Ando, Nat. Mater. **3**, 868 (2004).
[5]S. A. Wolf, D. D. Awschalom, R. A. Buhrman, J. M. Daughton, S. von Molnár, M. L. Roukes, A. Y. Chtchelkanova, and D. M. Treger, Science **294**, 1488 (2001).
[6]E. Cobas, A. L. Friedman, O. M. J. van't Erve, J. T. Robinson, and B. T. Jonker, Nano Lett. **12**, 3000 (2012).
[7]A. Bedoya-Pinto, M. Donolato, M. Gobbi, L. E. Hueso, and P. Vavassori, Appl. Phys. Lett. **104**, 062412 (2014).
[8]S. Yuasa, T. Nagahama, and Y. Suzuki, Science **297**, 234 (2002).
[9]J. S. Moodera, J. Nowak, L. R. Kinder, P. M. Tedrow, R. J. M. van de Veerdonk, B. A. Smits, M. van Kampen, H. J. M. Swagten, and W. J. M. de Jonge, Phys. Rev. Lett. **83**, 3029 (1999).
[10]P. LeClair, B. Hoex, H. Wieldraajjer, J. T. Kohlhepp, H. J. M. Swagten, and W. J. M. de Jonge, Phys. Rev. B **64**, 100406(R) (2001).
[11]I. J. Vera Marún, F. M. Postma, J. C. Lodder, and R. Jansen, Phys. Rev. B **76**, 064426 (2007).
[12]C. W. Miller, Z.-P. Li, I. K. Schuller, R. W. Dave, J. M. Slaughter, and J. Åkerman, Phys. Rev. Lett. **99**, 047206 (2007).
[13]L. Gao, X. Jiang, S. H. Yang, J. D. Burton, E. Y. Tsymbal, and S. S. P. Parkin, Phys. Rev. Lett. **99**, 226602 (2007).
[14]J. M. Rondinelli, M. Stengel, and N. A. Spaldin, Nat. Nanotechnol. **3**, 46 (2008).
[15]H. Kaiju, S. Fujita, T. Morozumi, and K. Shiiki, J. Appl. Phys. **91**, 7430 (2002).
[16]P. Padhan, P. LeClair, A. Gupta, K. Tsunekawa, and D. Djayaprawira, Appl. Phys. Lett. **90**, 142105 (2007).
[17]S. Ingvarsson, M. Arikan, M. Carter, W. F. Shen, and G. Xiao, Appl. Phys. Lett. **96**, 232506 (2010).
[18]A. M. Sahadevan, K. Gopinadhan, C. S. Bhatia, and H. Yang, Appl. Phys. Lett. **101**, 162404 (2012).
[19]Y.-M. Chang, K.-S. Li, H. Huang, M.-J. Tung, S.-Y. Tong, and M.-T. Lin, J. Appl. Phys. **107**, 093904 (2010).
[20]P. LeClair, J. T. Kohlhepp, A. A. Smits, H. J. M. Swagten, B. Koopmans, and W. J. M. de Jonge, J. Appl. Phys. **87**, 6070 (2000); K. S. Yoon, J. H. Park, J. H. Choi, J. Y. Yang, C. H. Lee, C. O. Kim, J. P. Hong, and T. W. Kang, Appl. Phys. Lett. **79**, 1160 (2001).
[21]See supplementary material at http://dx.doi.org/10.1063/1.4960202 for the standard dc-transport measurements, Cole-Cole plots, extraction of frequency independent fitting parameters, and other controlled experiments to establish different frequency responses.
[22]M. Jullière, Phys. Lett. A **54**, 225 (1975).
[23]B. G. Park, T. Banerjee, J. C. Lodder, and R. Jansen, Phys. Rev. Lett. **99**, 217206 (2007).
[24]S. Zhang, P. M. Levy, A. C. Marley, and S. S. P. Parkin, Phys. Rev. Lett. **79**, 3744 (1997).
[25]W. C. Chien, C. K. Lo, L. C. Hsieh, Y. D. Yao, X. F. Han, Z. M. Zeng, T. Y. Peng, and P. Lin, Appl. Phys. Lett. **89**, 202515 (2006); L. C. Hsieh, Y. W. Huang, X. F. Han, Z. M. Zeng, W. C. Chien, T. Y. Peng, C. K. Lo, and Y. D. Yao, J. Magn. Magn. Mater. **310**, 1903–1904 (2007).
[26]G. Landry, Y. Dong, J. Du, X. Xiang, and J. Q. Xiao, Appl. Phys. Lett. **78**, 501 (2001).
[27]J. Hampton, J. Eisenstein, L. Pfeiffer, and K. West, Solid State Commun. **94**, 559 (1995).
[28]T. Jungwirth and L. Smrčka, Phys. Rev. B **51**, 10181 (1995).
[29]S. Zhang, Phys. Rev. Lett. **83**, 640 (1999).
[30]K. T. McCarthy, A. F. Hebard, and S. B. Arnason, Phys. Rev. Lett. **90**, 117201 (2003).
[31]M. Gobbi, L. Pietrobon, A. Atxabal, A. Bedoya Pinto, X. Sun, F. Golmar, R. Llopis, F. Casanova, and L. E. Hueso, Nat. Commun. **5**, 4161 (2014).
[32]S. Parui, A. Atxabal, M. Ribeiro, A. Bedoya-Pinto, X. Sun, R. Llopis, F. Casanova, and L. E. Hueso, Appl. Phys. Lett. **107**, 183502 (2015).